Effects of the Photooxidant on DNA-Mediated Charge Transport

Tashica T. Williams, Chikara Dohno, Eric D. A. Stemp, and Jacqueline K. Barton*

*Contribution from the Division of Chemistry and Chemical Engineering,
California Institute of Technology, Pasadena, California 91125*

Received January 8, 2004; E-mail: jkbarton@caltech.edu

Abstract: A direct comparison of DNA charge transport (CT) with different photooxidants has been made. Photooxidants tested include the two metallointercalators, $Rh(phi)_2(bpy')^{3+}$ and $Ru(phen)(bpy')(dppz)^{2+}$, and three organic intercalators, ethidium (Et), thionine (Th), and anthraquinone (AQ). CT has been examined through a DNA duplex containing an A_6-tract intervening between two 5′-CGGC-3′ sites with each of the photooxidants covalently tethered to one end of the DNA duplex. CT is assayed both through determination of the yield of oxidative guanine damage and, in derivative DNA assemblies, by analysis of the yield of a faster oxidative trapping reaction, ring opening of N^2-cyclopropylguanine ($d^{CP}G$) within the DNA duplex. We find clear differences in oxidative damage ratios at the distal versus proximal 5′-CGGC-3′ sites depending upon the photooxidant employed. Importantly, nondenaturing gel electrophoresis data demonstrate the absence of any DNA aggregation by the DNA-bound intercalators. Hence, differences seen with assemblies containing various photooxidants cannot be attributed to differential aggregation. Comparisons in assemblies using different photooxidants thus reveal characteristics of the photooxidant as well as characteristics of the DNA assembly. In the series examined, the lowest distal/proximal DNA damage ratios are obtained with Ru and AQ, while, for both Rh and Et, high distal/proximal damage ratios are found. The oxidative damage yields vary in the order Ru > AQ > Rh > Et, and photooxidants that produce higher distal/proximal damage ratios have lower yields. While no oxidative DNA damage is detected using thionine as a photooxidant, oxidation is evident using the faster cyclopropylguanosine trap; here, a complex distance dependence is found. Differences observed among photooxidants as well as the complex distance dependence are attributed to differences in rates of back electron transfer (BET). Such differences are important to consider in developing mechanistic models for DNA CT.

Introduction

Oxidative damage to DNA promoted from a distance through DNA-mediated charge transport (CT) from a remotely bound photooxidant has, by now, been demonstrated and confirmed using a variety of photooxidants.[1-10] Hole transport from DNA-bound photooxidants can lead to oxidative damage at guanine sites, in particular at the 5′-G of 5′-GG-3′ doublets.[11] Indeed, reaction at the 5′-G of guanine doublets has become the signature for long-range oxidation by CT. DNA-mediated oxidative damage has been demonstrated over a distance of 200 Å.[12,13] While the reaction can, therefore, occur over long molecular distances, it is exquisitely sensitive to intervening sequence-dependent DNA structure. Intervening mismatches can attenuate oxidative damage through long-range CT,[14] as can protein binding[15,16] that perturbs the intervening base pair stack. In fact, the sensitivity of long-range CT to perturbations in base pair stacking has led to the development of electrochemical sensors for mutations, lesions, and protein binding.[17-20] Oxidative damage to DNA from a distance has been demonstrated

(1) Hall, D. B.; Holmlin, R. E.; Barton, J. K. *Nature* **1996**, *382*, 731–735.
(2) Saito, I.; Takayama, M.; Sugiyama, H.; Nakatani, K.; Tsuchida, A.; Yamamoto, M. *J. Am. Chem. Soc.* **1995**, *117*, 6406–6407.
(3) (a) Hall, D. B.; Kelley, S. O.; Barton, J. K. *Biochemistry* **1998**, *37*, 15933–15940. (b) Kurbanyan, K.; Nguyen, K. L.; To, P.; Rivas, E. V.; Lueras, A. M. K.; Kosinski, C.; Steryo, M.; González, A.; Mah, D. A.; Stemp, E. D. A. *Biochemistry* **2003**, *42*, 10269–10281.
(4) Gasper, S. M.; Schuster, G. B. *J. Am. Chem. Soc.* **1997**, *119*, 12762–12771.
(5) Nakatani, K.; Dohno, C.; Saito, I. *J. Am. Chem. Soc.* **1999**, *121*, 10854–10855.
(6) Giese, B. *Acc. Chem. Res.* **2000**, *33*, 631–636.
(7) Arkin, M. R.; Stemp, E. D. A.; Pulver, S. C.; Barton, J. K. *Chem. Biol.* **1997**, *4*, 389–400.
(8) (a) Stemp, E. D. A.; Arkin, M. R.; Barton, J. K. *J. Am. Chem. Soc.* **1997**, *119*, 2921–2925. (b) Nguyen, K. L.; Steryo, M.; Kurbanyan, K.; Nowitzki, K. M.; Butterfield, S. M.; Ward, S. R.; Stemp, E. D. A. *J. Am. Chem. Soc.* **2000**, *122*, 3585–3594.
(9) Wagenknecht, H.-A.; Rajski, S. R.; Pascaly, M.; Stemp, E. D. A.; Barton, J. K. *J. Am. Chem. Soc.* **2001**, *123*, 4400–4407.
(10) Pascaly, M.; Yoo, J.; Barton, J. K. *J. Am. Chem. Soc.* **2002**, *124*, 9083–9092.
(11) Sugiyama, H.; Saito, I. *J. Am. Chem. Soc.* **1996**, *118*, 7063–7068.

(12) Nùñez, M. E.; Hall, D. B.; Barton, J. K. *Chem. Biol.* **1999**, *6*, 85–97.
(13) Henderson, P. T.; Jones, D.; Hampikian, G.; Kan, Y.; Schuster, G. B. *Proc. Natl. Acad. Sci. U.S.A.* **1999**, *96*, 8353–8358.
(14) Bhattacharya, P. K.; Barton, J. K. *J. Am. Chem. Soc.* **2001**, *123*, 8649–8656.
(15) Rajski, S. R.; Kumar, S.; Roberts, R. J.; Barton, J. K. *J. Am. Chem. Soc.* **1999**, *121*, 5615–5616.
(16) Rajski, S. R.; Barton, J. K. *Biochemistry* **2001**, *40*, 5556–5564.
(17) Kelley, S. O.; Boon, E. M.; Barton, J. K.; Jackson, N. M.; Hill, M. G. *Nucleic Acids Res.* **1999**, *27*, 4830–4837.
(18) Boon, E. M.; Ceres, D. M.; Drummond, T. G.; Hill, M. G.; Barton, J. K. *Nat. Biotechnol.* **2000**, *18*, 1096–1100.
(19) Boon, E. M.; Salas, J. E.; Barton, J. K. *Nat. Biotechnol.* **2002**, *20*, 282–286.
(20) Drummond, T. G.; Hill, M. G.; Barton, J. K. *Nat. Biotechnol.* **2003**, *21*, 1192–1199.

within cell nuclei[21] and within DNA packaged in nucleosomes.[22] The sensitivity of DNA CT chemistry to mismatches and lesions has furthermore prompted the proposal that DNA repair enzymes may exploit DNA CT in detecting their targets within the cell.[23]

Oxidative damage from a distance through DNA CT was first demonstrated using a phenanthrenequinone diimine (phi) complex of rhodium(III) as the tethered intercalating photooxidant in DNA assemblies, where the metallointercalator was spatially separated from two 5′-GG-3′ doublets.[1] Thereafter, organic intercalators such as naphthalene diimide (NDI),[2] ethidium,[3] and modified anthraquinones[4] were also used to promote long-range oxidative DNA damage. Modified nucleotides such as 5-cyanobenzene deoxyuridine[5] and 4′-pivaloyl deoxythymine[6] have, in addition, been photolyzed to generate hot base and sugar radicals, respectively, that lead to oxidative damage at guanine sites from a remote position. A ground-state ruthenium(III) oxidant, containing the dipyridophenazine (dppz) ligand as the intercalating ligand and generated in situ in a flash-quench reaction, has, in addition to oxidative studies, been particularly valuable in spectroscopic measurements of the formation of radical intermediates at long range through DNA CT.[7−10]

These studies of oxidative damage have been utilized in developing mechanistic proposals for how DNA CT proceeds. The chemistry is currently viewed as involving a mixture of hopping and tunneling.[12,24,25] Owing to the sensitivity of DNA CT to the dynamical structure of DNA, we have considered DNA CT in terms of *domain hopping*, that is, hopping among DNA domains defined dynamically as stacked regions within the duplex through which charge is delocalized.[25c,26]

Given this mechanistic perspective, DNA CT is expected to be a characteristic of the DNA helix. Hence, while differences in oxidative damage may arise as a function of variations in intervening sequence and structure, results were expected basically to be similar irrespective of the oxidant employed. To account for differences in the efficiency of photoreaction, studies employed measurements of oxidative damage at distal versus proximal guanine sites as a means of normalization. Within such a framework, distal/proximal damage ratios were considered to be independent of the remotely bound oxidant employed. Moreover, these distal/proximal ratios were expected to have values of ≤ 1. Studies of oxidative damage using the rhodium photooxidant, however, revealed damage ratios consistently higher than 1; in the case of CT across an adenine tract, particularly high damage ratios of 3.5 were obtained.[26] These high damage ratios were explained in part as owing to the high longitudinal polarizability of DNA and the resultant effect of the high charge of the pendant Rh(III) photooxidant on the relative oxidation potentials of proximal versus distal 5′-GG-3′ sites.[27]

In multiply stranded DNA crossover assemblies, Sen and co-workers reported differing oxidation patterns using the rhodium intercalator versus anthraquinone as the photooxidant.[28] They accounted for these differences by arguing that the rhodium intercalators, once tethered, promote DNA aggregation, and hence oxidative damage yields were not wholly the result of oxidation by a remotely bound intercalator within one assembly but also arose owing to interassembly reactions. In support of this aggregation, nondenaturing gels were utilized to show a small percentage of a lower mobility band in the rhodium crossover assemblies. Importantly, conditions differed considerably from those utilized in earlier tests of oxidative damage using rhodium intercalators owing to the need for large concentrations of Mg^{2+} to maintain the crossover structures. Controls for intermolecularity were not carried out in these crossover studies also in contrast to all earlier studies of DNA CT in our laboratory. Moreover, the slow mobility band was neither characterized nor systematically examined as a function of concentration or incubation time. Schuster and co-workers then examined oxidative damage in a duplex assembly containing the repetitive adenine tract using the modified anthraquinone as the photooxidant, and they reported a distal/proximal oxidative damage ratio of 0.1.[29] Based on that data point, they have now proposed that all oxidative damage studies with all metallointercalators be considered difficult to interpret and problematic at best. It is, however, very difficult to understand how this aggregation model can account for the sensitivity of long-range oxidative DNA damage to intervening mismatches[14] or protein binding[15] and how this aggregation has not been revealed in detailed control measurements of intermolecularity.

These rationalizations and extrapolations concerning our studies of long-range oxidative damage with metallointercalators prompted us to examine in detail the possibility of aggregation by metallointercalators. It is noteworthy that detailed NMR studies had already been conducted that showed the *anticooperative* binding of metallointercalators to DNA.[30] Additionally, these proposals prompted us to carry out a direct comparison of oxidative damage using various photooxidants for the first time. Here, therefore, we compare reactions with different photooxidants directly. Indeed we do find clear differences in oxidative damage ratios depending upon the photooxidant employed. We provide additional data that demonstrate the absence of any DNA aggregation by the DNA-bound metallointercalators under the conditions used for photooxidation studies. Furthermore, using guanine derivatives that allow hole trapping to form irreversible oxidation products on a fast time scale, we provide evidence that the differences in oxidative damage ratios may depend on differences in rates of back electron transfer (BET) for different photooxidants. Such differences are important to consider in interpreting past and developing future models for DNA CT.

Experimental Section

Oligonucleotide Synthesis. Oligonucleotides were synthesized utilizing standard phosphoramidite chemistry on an ABI 392 DNA/

(21) Nùñez, M. E.; Holmquist, G. P.; Barton, J. K. *Biochemistry* **2001**, *40*, 12465−12471.
(22) Nùñez, M. E.; Noyes, K. T.; Barton, J. K. *Chem. Biol.* **2002**, *9*, 403−415.
(23) Boon, E. M.; Livingston, A. L.; Chmiel, N. H.; David, S. S.; Barton, J. K. *Proc. Natl. Acad. Sci. U.S.A.* **2003**, *100*, 12543−12547.
(24) (a) Giese, B. *Annu. Rev. Biochem.* **2002**, *71*, 51−70. (b) Schuster, G. B. *Acc. Chem. Res.* **2000**, *33*, 253−260. (c) Delaney, S.; Barton J. K. *J. Org. Chem.* **2003**, *68*, 6475.
(25) (a) Renger, T.; Marcus, R. A. *J. Phys. Chem. A* **2003**, *107*, 8404−8419. (b) Bixon, M.; Jortner, J. *Chem. Phys.* **2002**, *281*, 393−408. (c) Grozema, F. C.; Berlin, Y. A.; Siebbeles, L. D. A. *J. Am. Chem. Soc.* **2000**, *122*, 10903−10909.
(26) Williams, T. T.; Odom, D. T.; Barton, J. K. *J. Am. Chem. Soc.* **2000**, *122*, 9048−9049.
(27) Williams, T. T.; Barton, J. K. *J. Am. Chem. Soc.* **2002**, *124*, 1840−1841.

(28) Fahlman, R. P.; Sharma, R. D.; Sen, D. *J. Am. Chem. Soc.* **2002**, *124*, 12477−12485.
(29) Santhosh, U.; Schuster, G. B. *J. Am. Chem. Soc.* **2002**, *124*, 10986−10987.
(30) Franklin, S. J.; Treadway, C. R.; Barton, J. K. *Inorg. Chem.* **1998**, *37*, 5198−5210.

RNA synthesizer.[31] DNA was synthesized with a 5′-dimethoxy trityl (DMT) protecting group and purified on a Dynamax 300 Å C$_4$ reverse phase column (Rainin) (100% 50 mM NH$_4$OAc, pH 7, to 70% 50 mM NH$_4$OAc/ 30% acetonitrile over 35 min) on a Hewlett-Packard 1100 HPLC. 2-Fluoro-O^6-nitrophenyldeoxyinosine-containing strands, also containing a 5′-dimethoxy group, on solid support were treated with a 0.5 M DBU solution in acetonitrile for 20 min at ambient temperature, washed with additional acetonitrile, and treated with a 1% solution of triethylamine in acetonitrile. The strands were then treated with 6 M aqueous cyclopropylamine and heated at 60° C for 16 h to generate the d^{CP}G-containing DNA strands. The solution was filtered and concentrated to dryness. The isolated strands were then further treated with 80% glacial acetic acid and purified by reversed phase HPLC on a Microsorb C$_{18}$ column (10 × 250 mm^2; elution with 98% 50 mM NH$_4$OAc/2% acetonitrile to 88% 50 mM NH$_4$OAc/12% acetonitrile over 30 min). All strands were quantified using UV−visible spectroscopy on a Beckman DU 7400 spectrophotometer; ϵ_{260} (M^{-1} cm^{-1}) adenine = 15 400, guanine = 11 500, cytosine = 7400, thymine = 8700.

Preparation of oligonucleotides appended with rhodium, ruthenium, ethidium, and anthraquinone have been described elsewhere.[4,32−33] The modified DNA's were purified on a Dynamax C$_4$ column by reverse phase HPLC (95% 50 mM NH$_4$OAc (pH 7)/5% acetonitrile to 85% 50 mM NH$_4$OAc/ 15% acetonitrile over 45 min). In the case of the ruthenium and rhodium appended oligonucleotides, the Δ stereoisomer, established by circular dichroism (AVIV CD spectrophotometer), was used. All strands were characterized by MALDI-TOF or ESI mass spectrometry and UV−visible spectroscopy.

Synthesis of Thionine-Modified DNA. A. Preparation of N^3-Octanoic-Acid-Modified Thionine (1). A mixture of thionine (1.31 g, 4.54 mmol) and 8-bromooctanoic acid (1.51 g, 6.76 mmol) in DMF (20 mL) was refluxed for 6 h. The reaction mixture was concentrated in vacuo, and the residue was dissolved in methanol and filtered through Celite. The crude product was purified by column chromatography on silica gel (chloroform/methanol/acetic acid = 100:12:1.2) to give **1** (148.1 mg, 9%): ^{1}H NMR (CD3OD, 300 MHz) δ 1.38−1.73 (10H), 2.23 (m, 2H), 3.45 (m, 2H), 7.10−7.23 (4H), 7.86−7.89 (2H); ESI MS m/z 370.2 (M$^+$).

B. Preparation of N-Hydroxysuccinimidyl Ester of 1 (2). To a mixture of DCC (18.4 mg, 0.089 mmol) and hydrogen chloride salt of **1** (17.5 mg, 0.043 mmol) in dry DMF (1 mL) was added N-hydroxysuccinimide (10.1 mg, 0.088 mmol). The mixture was stirred at ambient temperature for 2 days under nitrogen. The solvent was removed in vacuo, and the crude product was purified by column chromatography on silica gel (chloroform/methanol/acetic acid = 100:12:1.2) to give **2** (14.0 mg, 0.028 mmol, 65%): ^{1}H NMR (CD3OD, 300 MHz) δ 1.36−1.74 (10H), 2.63 (t, 2H, J = 7.1 Hz), 2.81 (s, 4H), 3.44 (m, 2H), 7.06−7.20 (4H), 7.82−7.85 (2H); ESIMS m/z 467.2 (M$^+$); UV−vis (50 mM NaCl, 10 mM sodium phosphate (pH 7.0)) 619 nm, 286 nm.

C. Preparation of Thionine−DNA Conjugates. The synthesis of thionine−DNA conjugates was accomplished by the coupling of the succinimidyl ester of modified thionine (**2**) with 5′-alkylamino DNA. The 5′-alkylamino DNA was prepared by standard phosphoramidite synthesis followed by functionalization with hexamethylenediamine. To a DMF solution of activated ester (**2**) was added the 5′-alkylamino DNA in sodium phosphate buffer (pH 8.0), and the solution was kept at an ambient temperature for 2 h. The reaction mixture was purified on a Sep-Pack cartridge followed by reversed phase HPLC. All strands were confirmed by MALDI-TOF mass spectrometry and were all within 2 mass units of the calculated values.

(31) Beaucage, S. L.; Caruthers, M. H. *Tetrahedron Lett.* **1981**, *22*, 1859−1862.
(32) Holmlin, R. E.; Dandliker, P. J.; Barton, J. K. *Bioconjugate Chem.* **1999**, *10*, 1122−1130.
(33) Kelley, S. O.; Holmlin, R. E.; Stemp, E. D. A.; Barton, J. K. *J. Am. Chem. Soc.* **1997**, *119*, 9861−9870.

Assay of Oxidative DNA Damage. The oligonucleotides were labeled at the 5′-end utilizing γ-^{32}P-ATP and polynucleotide kinase.[34] After desalting, the reaction mixture was purified on a 20% denaturing polyacrylamide gel. The desired band was excised from the gel, soaked in 1 mL of 10 mM Tris-Cl and 1 mM EDTA (pH 7.5), dried in vacuo, and isolated by use of Micro Bio-Spin columns. Duplexes were prepared by mixing equimolar amounts of modified and unmodified strands to a final concentration of 2 μM, determined spectrophotometrically, and annealed in 20 mM Tris-Cl (pH 8.1) and 10 mM NaCl by heating to 90° C for 5 min and gradually cooling to ambient temperature over 2 h. For direct strand cleavage experiments, samples (30 μL) were irradiated at 313 nm for 10 min using a 1000 W Hg/Xe lamp equipped with a monochromator and immediately dried following irradiation. For oxidative damage experiments, parallel samples were irradiated at 365 nm for 1 h, treated with 10% piperidine (v/v), heated for 30 min at 90° C, and dried in vacuo. For the ruthenium-modified oligonucleotides (30 μL), irradiations were performed at 436 nm for either 1 h (without Co(NH$_3$)$_5$Cl^{2+}) or 10 min (with 25 μM Co(NH$_3$)$_5$Cl^{2+} (Aldrich)) and subsequently treated with 10% piperidine, heated to 90°C for 30 min, and dried. The ethidium- and anthraquinone-modified oligonucleotides were irradiated at 340 and 350 nm, respectively, for 1 h, and treated with piperidine as previously described. All samples were resuspended into formamide loading dye and electrophoresed through a 20% denaturing polyacrylamide gel. The extent of oxidative damage was determined by phosphorimagery (ImageQuant).

In determining the quantum yields, the extinction coefficients (M^{-1} cm^{-1}) were estimated to be the following for the respective oxidants: Rh, ϵ_{365} = 15 600; AQ-2, ϵ_{350} = 3000; Et, ϵ_{340} = 11 000; Ru-4, ϵ_{436}= 19 000. The lamp power was estimated to be 7 mW to 20 mW over the irradiation wavelengths of the oxidants. Sample volumes were 30 μL, and duplex concentrations were 2 μM.

Gel Electrophoresis under Nondenaturing Conditions. Parallel samples being used to test for oxidative damage were electrophoresed at 4 °C and 500 V for 24 h through a 20% nondenaturing gel containing 0.045 M Tris-borate (pH 8.3), 1 mM EDTA, and running dye. Subsequent analysis was performed utilizing phosphorimagery (ImageQuant).

Assay of Oxidative Damage with the d^{CP}G-Containing Duplexes. Duplexes were prepared by mixing equimolar amounts of modified and d^{CP}G-containing strands to a final concentration of either 2 μM or 5 μM and annealed in 20 mM Tris-Cl (pH 8.1) and 10 mM NaCl. Samples were irradiated for up to 60 min at the following wavelengths: AQ-2 at 350 nm; Rh at 365 nm; Ru at 436 nm; Et at 340 nm. After irradiation (20 μL), samples were fully digested with a mixture of alkaline phosphatase (33 units/mL), snake venom phosphodiesterase (3 units/mL), and nuclease P1 (33 units/mL) at 37 °C for 2 h. Digested solutions were analyzed by HPLC (C$_{18}$, 4.6 × 150 mm^2; elution with 98% 50 mM NH$_4$OAc/2% acetonitrile to 86% 50 mM NH$_4$OAc/14% acetonitrile over 30 min with a flow rate of 1 mL/min).

Results

Photooxidants and DNA Assembly. The photooxidants and DNA assembly examined are illustrated in Figure 1. Photooxidants tested include the two metallointercalators, Rh(phi)$_2$-(bpy′)$^{3+}$ and Ru(phen)(bpy′)(dppz)$^{2+}$, and three organic intercalators, ethidium (Et), thionine (Th), and anthraquinone (AQ), which was tethered in two ways (AQ-2 and AQ-5). We focused primarily on CT through a DNA duplex composed of an A$_6$-tract and two 5′-GG-3′ sites, since this sequence has been examined extensively and was found to be an effective medium for CT.[26] To provide a systematic comparison, all of the photooxidants were covalently tethered to one end of the DNA duplex. CT was assayed both through determination of the yield

(34) Sambrook, J.; Fritsch, E. F.; Maniatis, T. *Molecular Cloning: A Laboratory Manual*, 2nd ed.; Cold Spring Harbor Laboratory: New York, 1989.

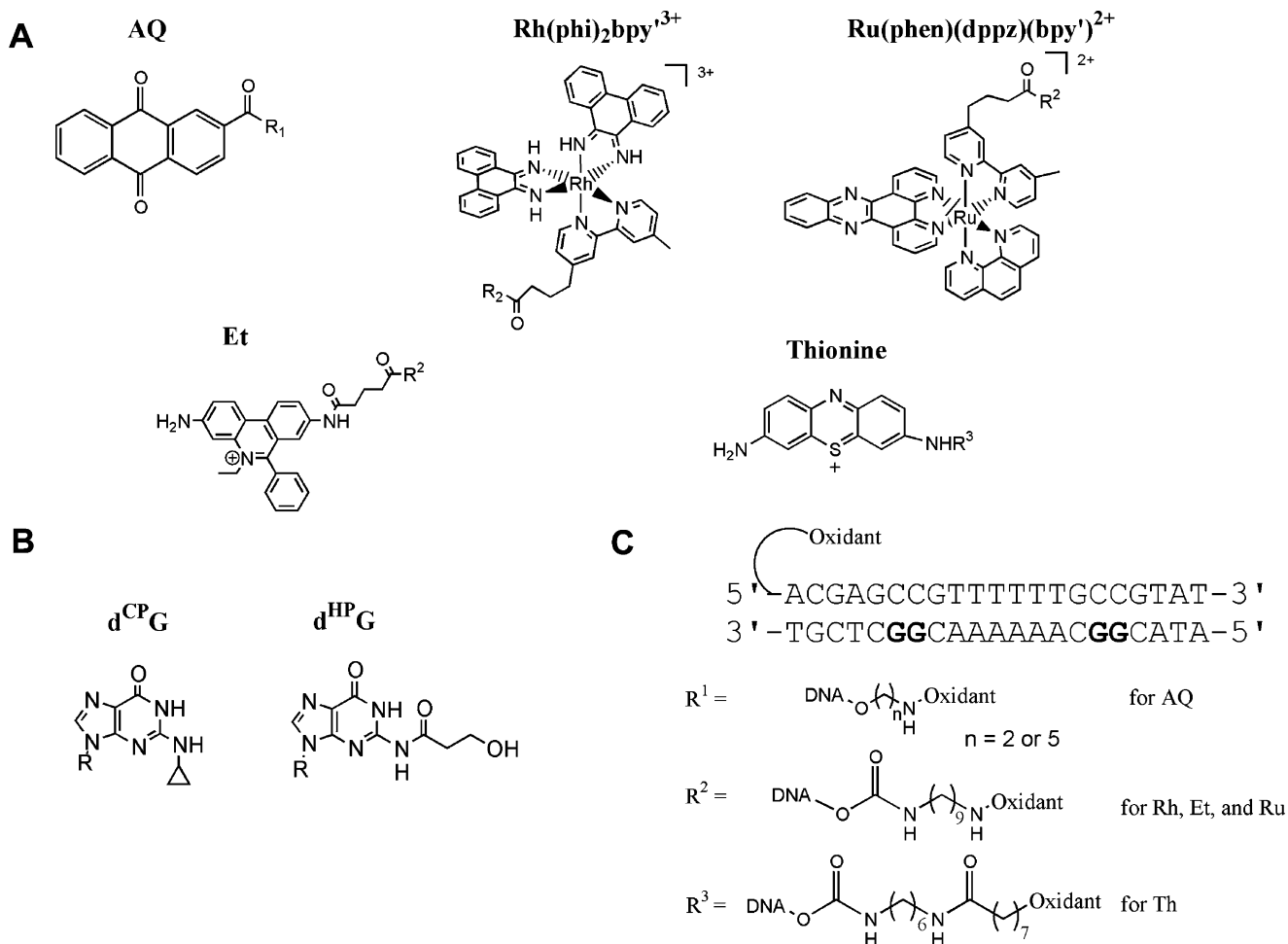**Figure 1.** Photooxidants, modified nucleosides, and the DNA assembly utilized in this work. (A) Clockwise from upper left: anthraquinone, Rh(phi)$_2$-(bpy')$^{3+}$, Ru(phen)(dppz)(bpy')$^{2+}$, thionine, and ethidium. (B) The modified nucleoside N^2-cyclopropylguanosine (left) and ring-opened product N^2-(3-hydroxypropanoyl)dG (right). (C) DNA assembly and functionalized linkers to the assembly.

of oxidative damage by PAGE analysis and by HPLC analysis of the yield of ring opening of N^2-cyclopropylguanine (d^{CP}G) within the DNA duplex. In the case of thionine, additional DNA duplexes were tested using the N^2-isopropylguanine trapping reaction.

Oxidative Damage Patterns of the Various Oxidants. Figure 2 shows the oxidative guanine damage that is revealed after 20% PAGE analysis of the photooxidant-tethered duplexes after irradiation and treatment of the DNA with piperidine (see Figure 1 for sequences of assemblies). For all of the photooxidants tested here, damage is found at 5′-GG-3′ sites both proximal and distal to the tethered oxidant. However both the extent of damage and relative damage at the proximal versus distal sites vary among the oxidants. Consistent with earlier reports,[26,29] a high distal/proximal guanine damage ratio is evident with Rh whereas a very low distal/proximal guanine damage ratio is found with AQ-2 and AQ-5. PAGE analysis of Ru-tethered duplexes (two Δ configurational isomers) show oxidative damage patterns that resemble those of the anthraquinone derivatives; appreciable damage is observed at the 5′-GG-3′ site that is proximal to the photooxidant, but little damage is seen at the distal 5′-GG-3′ site. Here oxidation is accomplished using the flash/quench reaction, where Ru(II) is photoexcited and oxidatively quenched by Co(NH$_3$)$_5$Cl^{2+} to generate Ru(III), the ground-state oxidant, in situ.[7,8] Not shown is reaction with

tethered thionine; we had earlier demonstrated that, despite the large driving force for photoreaction, no oxidative guanine damage is evident with thionine covalently or noncovalently bound to DNA.[35]

Also noteworthy is the direct strand photocleavage of DNA by tethered Rh upon irradiation at 313 nm. This direct strand cleavage chemistry marks the site of rhodium intercalation near the end of the duplex.[1] This direct cleavage chemistry has been utilized by us in all tests of oxidative reaction with Rh as a control to mark the rhodium binding site. Under the conditions in which we probe long-range oxidative damage, no cleavage is observed at sites other than near the duplex terminus where the Rh is tethered (Figure 2). Hence, these observations stand in contrast to a model of interduplex aggregation promoted by Rh under the conditions where long-range CT is probed.[28]

Ethidium, once tethered and irradiated at 340 nm, shows an oxidative damage pattern resembling that of Rh (Figure 2B). An appreciable amount of long-range oxidative guanine damage is observed at the distal 5′-GG-3′ site compared to the proximal site. Here damage is also observed at the guanine located near the duplex terminus where the Et is tethered. We have attributed

(35) Dohno, C.; Stemp, E. D. A.; Barton, J. K. *J. Am. Chem. Soc.* **2003**, *125*, 9586−9587.
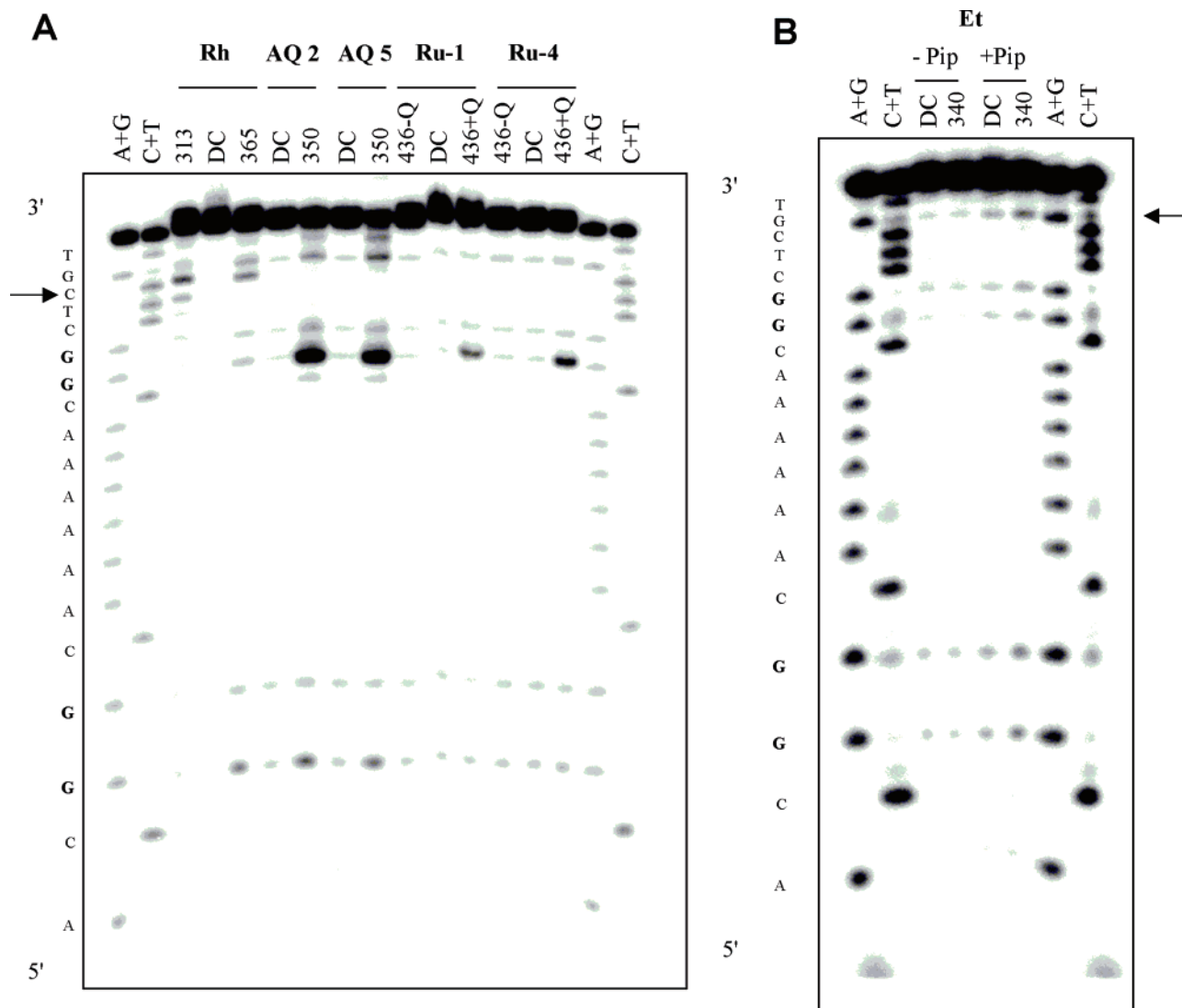
Figure 2. Oxidative damage with different photooxidants. 20% PAGE after irradiation of functionalized 5′-³²P-labeled DNA assemblies containing (A) Δ-Rh(phi)₂bpy′³⁺, AQ-2, AQ-5 and the Δ-1 and Δ-4 isomers (order of elution from HPLC) of Ru(phen)(dppz)(bpy′)²⁺, and (B) Et, respectively. The numbers above the lanes indicate the wavelength of irradiation. A + G and C + T are Maxam−Gilbert sequencing lanes. In part A, following irradiation, samples were treated with 10% piperidine (v/v), heated for 30 min at 90 °C, and dried; the 313 lane was not treated with piperidine. The 313 nm lane shows direct strand cleavage by Δ-Rh(phi)₂bpy′³⁺ after 10 min of irradiation at 313 nm; the arrow to the left indicates the site of direct cleavage marking the Rh intercalation. In all cases, lane DC indicates the dark control, which is the functionalized assembly without irradiation but with subsequent piperidine treatment. Lane 365 shows oxidative damage after irradiation of DNA functionalized with Δ-Rh(phi)₂bpy′³⁺ at 365 nm for 1 h. Lane 350 shows the oxidative damage yield after irradiation of both AQ-2 and AQ-5 assemblies for 1 h at 350 nm. Lanes 436 − Q and 436 + Q show oxidative damage after irradiation of DNA-tethered Ru(phen)(dppz)(bpy′)²⁺ at 436 nm for 1 h without Co(NH₃)₅Cl²⁺ and for 10 minutes with Co(NH₃)₅Cl²⁺ (25 μM), respectively. In part B, Et-functionalized asemblies are shown upon irradiation at 340 nm for 1 h with or without piperidine treatment. Here, direct cross-linking of the Et near the duplex terminus is indicated by the arrow. The concentrations for all of the assemblies were 2 μM duplex in 20 mM Tris-HCl (pH 8.1) and 10 mM NaCl.

this reaction to covalent cross-linking by the ethidium moiety.[3a,36] Also noteworthy here and consistent with earlier studies,[3] a high preference for the 5′-G of the guanine doublet is not found with Et; hole trapping studies with ᶜᴾG nonetheless support one-electron chemistry (*vide infra*).

Table 1 summarizes the distal/proximal DNA oxidation ratios for these tethered photooxidants on DNA assemblies of identical sequence. It is clear that different distal/proximal oxidation ratios are found depending upon the photooxidant employed. Notably Et, like Rh, yields high distal/proximal ratios whereas, for Ru or AQ, greater reaction is found at the proximal 5′-GG-3′ site compared to the distal site.

Also shown in Table 1 are estimates of the quantum yield for oxidative guanine damage, Φ(Gox), on these DNA assemblies. For all photooxidants, these values are low. These low yields are understandable given (i) irreversible oxidative guanine damage is at least two steps removed from guanine radical formation and (ii) the gel assay measures only the portion of that reaction that is piperidine sensitive.[1,12] The yields decrease with photooxidants as follows: Ru > AQ > Rh > Et. Notably, the highest efficiency reaction is obtained with the ruthenium oxidant, and in fact, if calculated versus Ru(III) oxidant generated in situ rather than per Ru(II), the value would be still higher. For Rh, the yield is approximately 1 order of magnitude lower than that for AQ, measured on DNAs of identical sequence using identical conditions. For Et a still lower

(36) Wan, C.; Fiebig, T.; Kelley, S. O.; Treadway, C. R.; Barton, J. K.; Zewail, A. H. *Proc. Natl. Acad. Sci. U.S.A.* **1999**, *96*, 6014−6019.

Table 1. Summary of the Oxidative Guanine Damage by Biochemical Analysis and ^{CP}G Consumption

photooxidant[a]	5′-GG-3′ D/P[b]	$\Phi\ G_{ox} \times 10^4$	$5'^{CP}$G D/P[h]
[Rh(phi)$_2$bpy′]$^{3+}$	1.4 (±0.2)	0.02	0.12
[Ru(phen)(dppz)(bpy′)]$^{2+}$	0.08 (±0.03)[c]	0.9[g]	0.03
	0.08 (±0.05)[d]		
AQ	0.07 (±0.02)[e]	0.2[i]	0.03[i]
	0.09 (±0.06)[f]		
Et′	1.5 (±0.3)	0.01	0.4[j]

[a] Photooxidants tethered to assemblies as shown in Figure 1. [b] Total amount of 5′-G and 3′-G oxidative guanine damage as observed by PAGE analysis at the distal (D) versus proximal (P) sites. The results reflect three to five trials for each. [c,d] (5′ + 3′) GG oxidative damage yields for Ru-1 and Ru-4 Δ isomers, respectively. [e,f] (5′ + 3′) GG oxidative damage yields for AQ modified DNA with $n=2$ and $n = 5$ methylene spacers, respectively. [g] This yield is determined per Ru(II) and is an underestimate versus Ru(III) oxidant generated using 25 μM Co(NH$_3$)$_5$Cl^{2+} as the quencher. [h] Consumption of the distal ^{CP}G versus 40% consumption of the ^{CP}G at the proximal site. [i] AQ-2 was utilized. [j] Consumption of the distal ^{CP}G versus 30% consumption of the ^{CP}G at the proximal site.
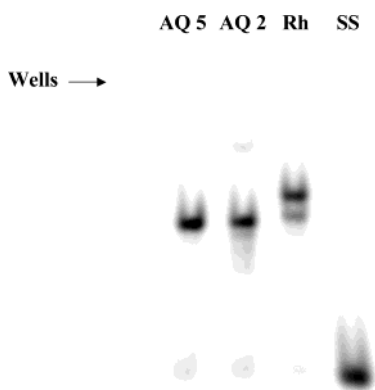
AQ 5   AQ 2   Rh   SS

Wells ⟶

Figure 3. 20% nondenaturing polyacrylamide gel electrophoresis of 5′-^{32}P-labeled DNA duplexes functionalized with AQ-2 (endcapped), AQ-5 (intercalated), or Δ-Rh(phi)$_2$bpy′$^{3+}$. Also shown is the single strand control (SS) for the 5′-^{32}P-labeled DNA without annealing to a functionalized complement. All samples were 2 μM duplex in 20 mM Tris-Cl (pH 8.1) and 10 mM NaCl. Note in the Rh lane the presence of two bands assigned to the two bound isomers of the Rh-functionalized DNA. In the AQ-2 lane, there is also a small percentage of a much slower mobility band.

yield is obtained. These differences can certainly be understood based upon a difference in rates of BET among the photooxidants (vide infra).

Native Gel Analysis of Photooxidant-Tethered Assemblies. As another test of possible aggregation of assemblies, we examined the mobility of the oxidant-tethered DNA using nondenaturing gel electrophoresis. As shown in Figure 3, under conditions and using samples tested also for oxidative damage, two duplex bands of similar mobility are found with the Rh-tethered assemblies and primarily one band of comparable mobility is evident with the AQ-modified duplexes. The two bands found with Rh, only distinguishable with very slow gel electrophoresis, are assigned to the two configurational isomers of the tethered complex. Both have mobilities slightly less than the AQ-functionalized DNA, consistent with the high positive charge on the Rh. Importantly, no significantly slow-moving band, as might be expected if two duplexes aggregated together, is evident with the Rh-tethered DNA. In fact, a very small intensity of a slow migrating band is observed only in the end-capped AQ-2 sample.

We also examined Et- and Ru-tethered assemblies by nondenaturing gel electrophoresis (data not shown). For these assemblies as well, no slow moving bands are evident. None

of these modifications lead to aggregation of DNA under conditions where long-range DNA CT is probed.

These results differ from those reported by Sen and co-workers in their studies of DNA crossover assemblies with tethered Rh. In an effort to understand the basis for their observations, we examined Rh-modified duplexes also under the high ionic strength conditions used to stabilize the DNA crossovers (0.04 M Tris-borate, 0.1 mM EDTA 2 mM Mg^{2+}). There, too, no low mobility bands are evident. We also tested the assemblies by nondenaturing electrophoresis with 2 mM Mg^{2+} within the gel. In this case, we sometimes observed a small percentage of a slow moving band, but this was not reproducible; we believe this result to be an artifact associated with loading the samples onto gels with high [Mg^{2+}]. Besides the high [Mg^{2+}] in solution samples and in the gels, another difference between our conditions and those utilized by Sen is that they appear to have first precipitated samples and carried out the electrophoresis experiments on a subsequent day. In our experiments, samples are not first precipitated and resuspended, and samples are never stored overnight before completing the experiment. For there to be a direct extrapolation to our studies, experiments clearly need to be performed under the same conditions.

Long-Range CT Studies with Thionine. Since we had earlier determined that photolysis of thionine yielded no detectable oxidative damage to DNA, we sought chemical evidence of long-range CT with this intercalating photooxidant. Toward that end, we synthesized d^{CP}G as described previously[37,38] and first examined the photooxidation of the d^{CP}G nucleoside by thionine. Irradiation was carried out at 599 nm aerobically in the presence of thionine, and the oxidation products were analyzed by HPLC. Upon irradiation, d^{CP}G was rapidly consumed, producing two major products. These two products were identified as dG and N^2-(3-hydroxypropanoyl)dG (d^{HP}G) by mass spectrometry and HPLC retention times and are fully consistent with previously observed one-electron oxidation products of d^{CP}G (Figure 4). The rapid consumption and the identical oxidation products indicate that the excited thionine surely produces d^{CP}G radical cation.

For further confirmation of one-electron oxidation chemistry, we also examined the effect of oxygen, since thionine is known to be a singlet oxygen generator.[39,40] Under anaerobic conditions, d^{CP}G was consumed with similar kinetics as in the presence of oxygen, but different products were generated (supporting). Since oxygen is considered to be involved in the mechanism of the formation of d^{HP}G under aerobic conditions, different products are expected in the absence of oxygen. Significantly, the similar consumption rate indicates that singlet oxygen is not responsible for the rapid consumption of d^{CP}G.

In contrast to the rapid decomposition of d^{CP}G, dG remains unchanged under the same reaction conditions (Figure 4). Although dG loses an electron to generate the dG radical cation in the presence of photoexcited thionine, we have recently shown that fast BET suppresses the decomposition of dG.[35] In that

(37) Nakatani, K.; Dohno, C.; Saito I. *J. Am. Chem. Soc.* **2001**, *123*, 9681–9682.
(38) Dohno, C.; Ogawa, A.; Nakatani, K.; Saito I. *J. Am. Chem. Soc.* **2003**, *125*, 10154–10155.
(39) (a) Tuite, E. M.; Kelly, J. M. *J. Photochem. Photobiol., B* **1993**, *21*, 103–124. (b) Tuite, E. M.; Kelly, J. M.; Beddard, G. S.; Reid, G. S. *Chem. Phys. Lett.* **1994**, *226*, 517–524.
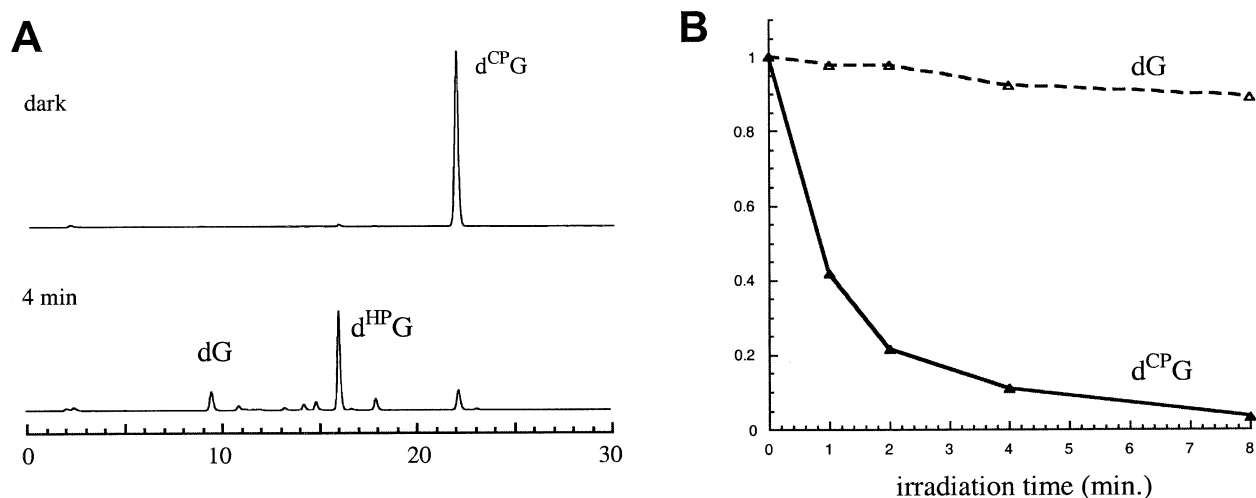(40) Saito, I.; Inoue, K.; Matsuura, T. *Photochem. Photobiol.* **1975**, *21*, 27–30.

A

B

Figure 4. (A) HPLC profiles of $d^{CP}G$ oxidation by photoexcited thionine. A solution of $d^{CP}G$ (250 μM) and thionine (25 μM) in 10 mM sodium phosphate (pH 7.6), 50 mM NaCl was irradiated at 599 nm for 4 min under aerobic conditions. (B) Time course of the amount of dG and $d^{CP}G$ remaining upon irradiation of each in the presence of thionine (25 μM).
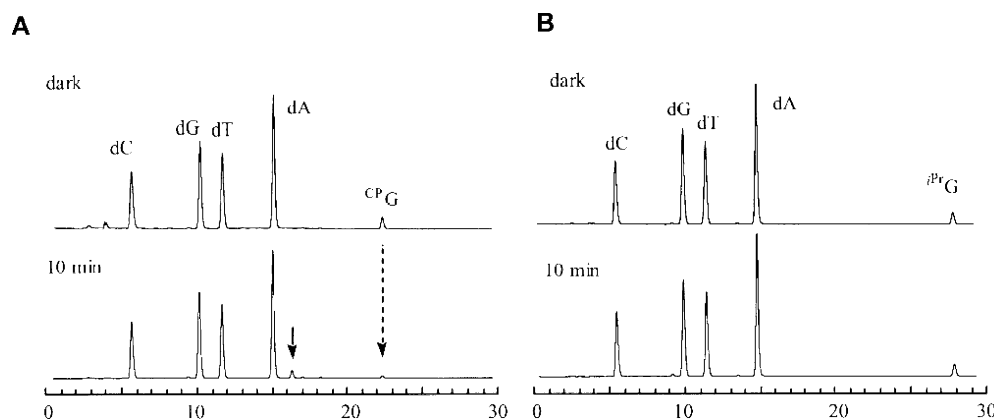
A   **B**

Figure 5. HPLC profiles of nucleoside mixtures obtained from the enzymatic digestion of the irradiated (A) $d^{CP}G$-containing-DNA/Th conjugate and (B) $d^{iPr}G$-containing/Th conjugate. The duplex (5 μM) in 10 mM sodium phosphate (pH 7.6), 50 mM NaCl was irradiated for 20 min at 599 nm under aerobic conditions, followed by enzymatic digestion.

case, fast BET conceals the evidence of electron transfer, the formation of oxidation products, since BET competes with the slow reaction of the guanine radical to form irreversible products. Reaction of $d^{CP}G$ reveals the occurrence of electron transfer, since rapid ring opening traps the hole on a time scale that is competitive with BET.

To establish CT between excited thionine and dG embedded in duplex DNA, we have also examined trapping of the radical cation by $d^{CP}G$-containing DNA. The $d^{CP}G$-containing DNA strands are hybridized with complementary thionine−DNA conjugates in which thionine is covalently tethered at the 5′-terminus of the DNA (Figure 1). The DNA duplexes were irradiated at 599 nm followed by enzymatic digestion to the nucleosides. HPLC traces (Figure 5A) of the nucleosides clearly show the consumption of $d^{CP}G$ accompanied by the formation of $d^{HP}G$. In contrast, when isopropylguanosine ($d^{iPr}G$) is incorporated instead of ^{CP}G, the amount of $d^{iPr}G$ does not vary after 60 min irradiation (Figure 5B). This indicates that hole trapping is based on the rapid ring opening of the attached cyclopropyl group, not the lowered oxidation potential of $d^{CP}G$ (−0.14 V compared to dG).[37,38] These results clearly demonstrate that excited thionine produces G radical cation from a distance via electron transfer through π-stacked DNA, even

though no evidence[35] of oxidative DNA damage is observed by gel electrophoresis.

So as to provide a comparison to our studies of distal/proximal oxidation ratios with other photooxidants, we were interested also in determining how the yield of the ring opening trapping reaction varies as a function of distance from the tethered thionine. Figure 6 includes several assemblies prepared with tethered thionine as well as the distance dependence of the ^{CP}G consumption in these assemblies. Overall, the consumption decreases with increasing distance between thionine and ^{CP}G. For example, in contrast to the rapid consumption of ^{CP}G in assembly **P**, the amount of ^{CP}G in assembly **6** remained almost unchanged after 60 min of irradiation. This is also the case for other DNA assemblies we have examined with a shorter distance between two GG sites (data not shown). These results indicate that BET from the proximal GG site is much faster than the rate of hole transport to the distal GG site.[41,42] Also notable is the observation that the $d^{CP}G$ consumption rate is lowered if a mismatched base pair (**M**) is introduced at the 3′-side of ^{CP}G intervening between the thionine and ^{CP}G. Likely, the significant

(41) Lewis. F. D.; Wu, T.; Letsinger, R. L.; Wasielewski, M. R. *Acc. Chem. Res.* **2001**, *34*, 159−170.
(42) The rate for hole hopping between two single Gs separated by two AT base pairs was estimated to be $\geq 10^6$ s^{-1}.[24]
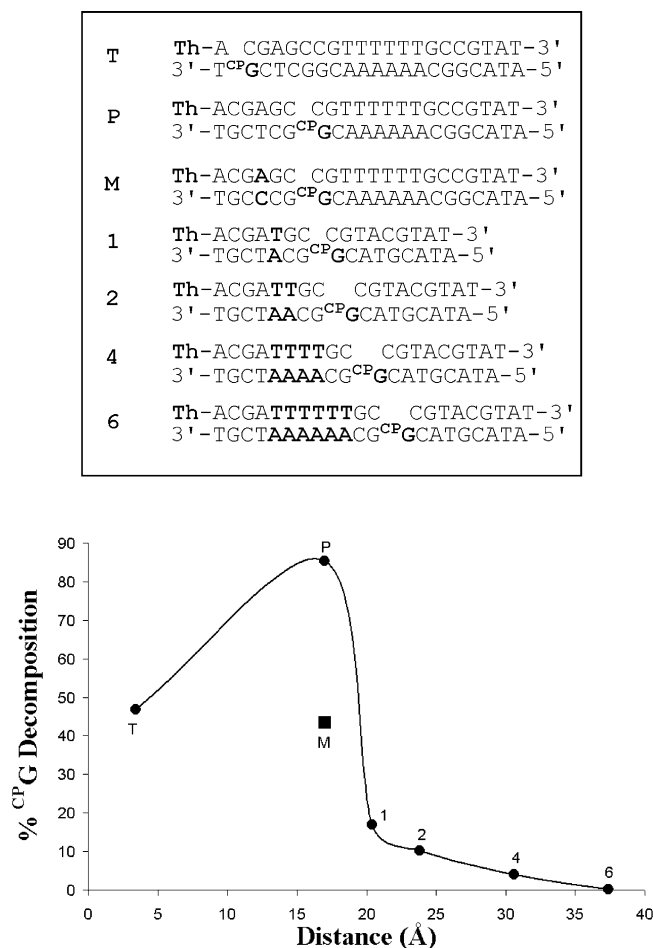
```
T    Th-A CGAGCCGTTTTTTGCCGTAT-3'
     3'-TCPGCTCGGCAAAAAACGGCATA-5'

P    Th-ACGAGC CGTTTTTTGCCGTAT-3'
     3'-TGCTCGCPGCAAAAAACGGCATA-5'

M    Th-ACGAGC CGTTTTTTGCCGTAT-3'
     3'-TGCCCGCPGCAAAAAACGGCATA-5'

1    Th-ACGATGC CGTACGTAT-3'
     3'-TGCTACGCPGCATGCATA-5'

2    Th-ACGATTGC  CGTACGTAT-3'
     3'-TGCTAACGCPGCATGCATA-5'

4    Th-ACGATTTTGC  CGTACGTAT-3'
     3'-TGCTAAAACGCPGCATGCATA-5'

6    Th-ACGATTTTTTGC  CGTACGTAT-3'
     3'-TGCTAAAAAACGCPGCATGCATA-5'
```


Figure 6. Consumption of $d^{CP}G$ in $d^{CP}G$-containing-DNA/Th conjugates as a function of distance separating $d^{CP}G$ and thionine. The sequences for the assemblies examined (top) and the plot of % $d^{CP}G$ consumption versus distance (bottom) are shown. In all cases, samples (5 μM) were irradiated for 10 min at 599 nm under aerobic conditions, followed by enzymatic digestion and HPLC analysis. Note that the presence of an intervening mismatch (M) attenuates the long-range CT reaction. Also note the complex distance dependence.

difference between **P** and **1** is also structural, given the intervening AT step for **1**.[12]

Interestingly, however, we also observe a slower consumption rate in assembly **T** than in assembly **P**, where ^{CP}G is located very close to the tethered thionine. This diminished reaction may in part be due to the lower oxidation potential of the GG doublet. However also another contribution to this lowered reaction at the near ^{CP}G may be that the ^{CP}G ring-opening rate is slower than the rate of BET in **T**; it is known that BET between thionine, noncovalently bound, and dG in poly d(GC) occurs on the femtosecond time scale.[39,43] Importantly an inverse distance dependence was observed for short distances in hole trapping studies[44] using photoexcited 2-aminopurine and in photooxidation studies[45] using NDI. We consider that the tethered thionine is intercalated close to the DNA terminus based upon modeling, based upon experimental data showing variations in oxidative damage with variation in the sequence near

(43) Reid, G. D.; Whittaker, D. J.; Day, M. A.; Turton, D. A.; Kayser, V.; Kelly, J. M.; Beddard, G. S. *J. Am. Chem. Soc.* **2002**, *124*, 5518−5527.
(44) O'Neill, M. A.; Dohno, C.; Barton, J. K. *J. Am. Chem. Soc.* **2004**, *126*, 1316−1317.
(45) Kawai, K.; Takada, T.; Nagai, T.; Cai, X.; Sugimoto, A.; Fujitsuka, M.; Majima, T. *J. Am. Chem. Soc.* **2003**, *125*, 16198−16199.

the terminus, and based upon damage of the analogous thionine-tethered DNA without ^{CP}G only at the G one base in from the terminus after extensive photolysis.[35]

Hole Trapping by ^{CP}G with Other Photooxidants. We also examined hole trapping of 5′-^{CP}G-containing DNA by the full family of photooxidants shown in Figure 1. As with bound thionine, the ^{CP}G-DNAs contained two 5′-GG-3 sites with an intervening A_6-tract, where one of the 5′-GG-3′ sites is replaced by 5′-^{CP}GG-3′. The consumption of ^{CP}G in each strand was analyzed by HPLC after enzymatic digestion to nucleosides. Typical HPLC profiles after photooxidation are shown in Figure 7 for AQ and Rh. With all of the photooxidants utilized, oxidation at the proximal 5′-^{CP}GG-3′ site produces the known product, $d^{HP}G$ (Figure 1). In contrast to rapid consumption of the proximal ^{CP}G, the distal ^{CP}G is consumed more slowly under the same reaction conditions, but yields the same product, $d^{HP}G$ (supporting). Note the smaller amount of $d^{HP}G$ with Rh and AQ compared to that with thionine. We attribute this difference to some decomposition of $d^{HP}G$ once formed, since with Rh and AQ some decomposition of dG is also always evident.

A study under anaerobic conditions was also performed utilizing AQ-2, since oxygen has been proposed to be a key participant in the long-range CT chemistry of AQ.[46] Deoxygenation does not significantly attenuate trapping by ^{CP}G at the proximal site, although a slight decrease in trapping of the ^{CP}G at the distal site is observed.

Table 1 also summarizes the distal/proximal ratio of reaction at 5′-^{CP}GG-3′ sites. Once again, Rh and Et yield higher 5′-^{CP}G distal/proximal ratios than observed for Ru or AQ. All values, however, reflect ratios that are <1. Furthermore, for all photooxidants, the yield of this trapping reaction is 2 orders of magnitude higher than oxidative damage yields. Moreover, as with measurements of oxidative damage, the yields decrease with photooxidants as follows: Ru ≥ AQ > Rh > Et.

Discussion

Tethered Metallointercalators Do Not Aggregate under Assay Conditions for DNA CT. The application of metallo-intercalators generally and rhodium intercalators specifically to probe long-range CT in DNA was called into question owing to the possibility of metal-promoted aggregation of DNA assemblies in solution.[28] Our experiments provide evidence against aggregation of metal-tethered DNA assemblies under the conditions where DNA CT studies are measured. We find no evidence of a slow moving species in nondenaturing gels as would be expected if aggregation were occurring. NMR results earlier established the sequence-neutral, anticooperative binding of noncovalently bound Rh and Ru intercalators to DNA, inconsistent with an aggregation model.[30] Furthermore concentration dependences of long-range DNA oxidative damage with tethered intercalators have been conducted as have mixed labeling experiments using oxidant-tethered assemblies lacking a radioactive tag mixed with DNA assemblies containing the radioactive tag but lacking the oxidant. These experiments have also always provided results that are *inconsistent* with an interduplex association.[1,7,12] Last, direct strand cleavage controls on Rh-tethered assemblies are *always* performed in our laboratory in each DNA CT investigation to mark the site of Rh

(46) Ly, D.; Kan, Y.; Armitage, B.; Schuster, G. B. *J. Am. Chem. Soc.* **1996**, *118*, 8747−8748.

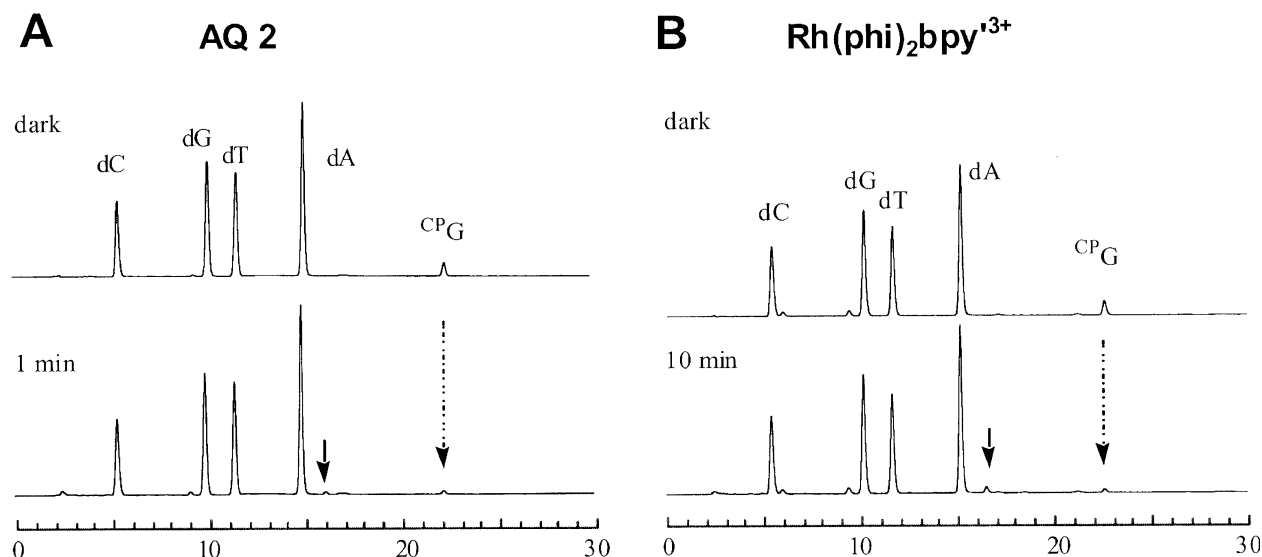**A**   **AQ 2**

B   **Rh(phi)₂bpy'³⁺**

Figure 7. HPLC profiles of nucleoside mixtures obtained from enzymatic digestion of irradiated ᶜᴾG-containing DNA assemblies functionalized with Rh and AQ. Results are shown for the assembly derivatized with ᶜᴾG at the proximal site. (A) The ᶜᴾG-DNA/AQ-2 duplex (5 μM) in 10 mM sodium phosphate (pH 7) was irradiated for 1 min at 350 nm followed by enzymatic digestion. (B) The ᶜᴾG/Rh assembly (5 μM) in 20 mM Tris-Cl (pH 8.1), 10 mM NaCl was irradiated at 365 nm for 10 min followed by enzymatic digestion.

binding on the assembly. This too necessarily establishes that the reaction is intraduplex, since, in these experiments, these data always reveal direct strand cleavage near the duplex terminus, the intercalator binding site if tethered to the same duplex, and no cleavage is found at other sites further along the duplex that cannot be accessed by Rh in an intraduplex association.

The suggestion that nondenaturing gels be included as another assay of the modified DNA assemblies is nonetheless a reasonable one, especially for DNA assemblies where the binding site cannot be marked discretely as it can with the Rh photochemistry. It is noteworthy that the position of intercalation is only precisely described for the Rh oxidant because of its unique direct strand cleavage photochemistry. In more recent investigations, we have been incorporating this additional gel control; studies of DNA CT in a DNA duplex/quadruplex assembly utilizing Rh(phi)₂bpy'³⁺ as the photooxidant also show no evidence of aggregating species in nondenaturing gels and clearly reveal one band due to the DNA duplex/quadruplex conjugate.[47] The aggregation studies performed by Sen and co-workers on DNA crossover assemblies[28] were not carried out under conditions we utilize to promote DNA CT generally, nor were they carried out in a systematic fashion. In fact, the yield of the slow moving band reported cannot even account for the oxidative DNA damage yields obtained in the DNA crossovers. How aggregation models can account for differences found in oxidative damage as a function of protein binding[15,16] or with intervening mismatches[14] is also difficult to understand.

The difference in oxidative damage yields and distal/proximal damage ratios using the photooxidants presented here is certainly therefore not the result of the aggregation of the metallointercalators. There are, nonetheless, significant differences among photooxidants, and this issue needs to be addressed. We propose that differing extents of BET can account for the differing extents of oxidative guanine damage that we observe here.

(47) Delaney, S.; Barton, J. K. *Biochemistry* **2003**, *42*, 14159−14165.

Differences in Both Yield and Distal/Proximal Damage Ratios Are Found To Depend on the Tethered Photooxidant. While differences seen with assemblies containing various photooxidants cannot be attributed to differential aggregation, there are clear differences among them. In fact, remarkably, these studies represent the first time where various photooxidants have been compared directly with respect to long-range DNA CT. In the series examined, the lowest distal/proximal ratios are obtained with Ru and AQ, while, for both Rh and Et, high distal/proximal damage ratios are found. In the case of thionine, calculation of the damage ratio is moot, since no oxidative damage is detected. Consistent with this finding, a correlation is seen between absolute yield of oxidative damage and distal/proximal ratio; photooxidants that produce higher damage yields overall give lower distal/proximal ratios (Table 1). Certainly these results establish that the use of distal/proximal damage ratios as a means of characterizing a given assembly with respect to efficiency of CT is valid only with a constant photooxidant. Comparisons in assemblies using different photooxidants reveal characteristics of the photooxidant as well as characteristics of the DNA assembly.

We first proposed that differences in the oxidative damage ratios may be based in part upon the high charge of the photooxidant affecting potentials at the proximal versus distal 5′-GG-3′ sites to a differing extent.[27] Here, however, the differing ratios do not correlate with different charges on the photooxidants. Aggregation has also been eliminated as a possible explanation for the differences. Additional factors must therefore govern these differing results.

Back Electron Transfer as a Distinguishing Characteristic of the Photooxidant. Another explanation rests in the differing rates of back electron transfer (BET) for the different photooxidants. It is known that trapping of the guanine radical cation to produce irreversible products is relatively slow compared to CT. Measurements of guanine radical decay by transient absorption spectroscopy reveal a decay time on the order of milliseconds.[8] Since oxidative damage measurements by gel
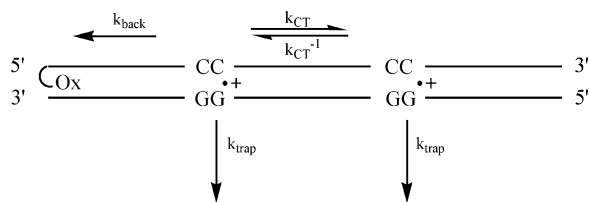
Figure 8. Schematic illustrating pathways for CT in oxidant-tethered assemblies.

electrophoresis only provide a static picture of the net product yield, certainly these yield measurements may be expected to differ based upon rates of BET.

Figure 8 shows the full scheme for hole equilibration across a DNA assembly. Several limiting conditions should be considered. First, if the trapping reaction is much slower than the rate of CT and the potentials on the distal and proximal 5′-GG-3′ guanine sites are the same, one would expect equal yield at distal and proximal sites, e.g., a distal/proximal damage ratio of 1. Conversely, if the rate of CT is limiting compared to the rate of trapping, reaction would be expected to be much greater at the proximal site, e.g., approaching a distal/proximal damage ratio of 0. As the rate of CT and rate of trapping become competitive, an intermediate distal/proximal ratio is expected.

These limiting cases, however, assume no contribution of BET. If the rate of BET is competitive with the rate of trapping but slower than CT, equilibration across the two sites would still hold. However, as the rate of BET increases compared to trapping, indeed as it approaches the rate of CT, reaction at the proximal site should be depleted. Hence high values of the distal/proximal damage ratio exceeding values of 1 would be expected. Indeed, with Rh and Et as photooxidants, this is what we observe.

In that context, thionine provides an example of an extreme. Despite a large driving force and evidence for reaction by CT chemistry, no oxidative DNA damage at either proximal or distal sites is detectable with photoexcited thionine.[35] However, fast BET in poly d(GC) by photoexcited thionine has been seen to proceed on the femtosecond time scale.[39,43−44] This rapid BET accounts for the absence of any detectable yield of oxidative DNA damage. If we examine reactions using a faster trap, however, as in the ring-opening reaction, now oxidation at a distance is evident. The overall yield of reaction necessarily depends on the rate of BET relative to the rate of trapping.

Perhaps more interesting is the distance dependence for this oxidation reaction viewed with the fast trap as illustrated in Figure 6. At long distances, where BET is slow, there is an understandable decrease in reaction with increasing distance; the slope of the efficiency of reaction with distance is negative, and any measure of a "distal/proximal" ratio would be <1. At a short distance, however, the opposite is seen. BET over this shorter distance range becomes comparable to CT and trapping; the slope of the efficiency of reaction with distance is positive, and a measure of a "distal/proximal" ratio in this regime would be >1. It should be noted that photoexcited 2-aminopurine similarly shows no yield in oxidative DNA damage, reflecting a high rate of BET, and with this photooxidant as well, an inverse distance dependence in cyclopropyl guanosine ring opening is found at short distances.[44] Furthermore, photo-oxidation experiments with NDI show guanine oxidation to correlate with the lifetime of the charge separated state and not the distance separating the oxidant and its substrate.[45]

The other photooxidants surely have BET rates slower than that of thionine since oxidative DNA damage can be seen. Nonetheless, as one would expect if BET is a dominating factor in comparing these photooxidants, their quantum yields for oxidative DNA damage vary in the order Ru > AQ > Rh > Et, and similarly the distal/proximal guanine damage ratios vary Ru = AQ < Rh < Et. Just as the quantum yields for oxidative damage for Rh and Et are lower than for Ru and AQ, the distal/proximal ratios are higher for Rh and Et versus Ru and AQ. Importantly, then, if rates of BET for the Rh and Et photooxidants approach rates of CT, then reaction with these oxidants at the proximal site is expected to be depleted, and distal/proximal damage ratios are expected to increase. Indeed, this is what we observe. Moreover, for Ru, a ground-state oxidant, little BET to the sacrificial quencher is expected, consistent with the highest yield for this reaction. Hence, faster rates of BET for Rh and Et relative to those for Ru and AQ account well for the differing ratios and quantum yields we observe.

It is worth noting that the energetics of the redox reactions for formation and disappearance of the guanine radical also support the idea that the kinetics of BET are fundamental in determining the yield of guanine damage at a distance. For Rh and AQ, oxidation of G is accomplished from the excited states, which have energies of +2.0 eV and +2.7 eV for photoexcited Rh[48] and AQ (triplet state),[49] respectively. The driving forces for photooxidation of G (1.3 V)[50] are 0.7 eV for Rh and 0.6 eV for AQ.[51] In the case of the reduction of one-electron oxidized guanine by the reduced intercalator (i.e., the back reaction), the driving force would be 1.3 eV for Rh and 2.1 eV for AQ. Estimates of the reorganization energy for DNA systems vary, but assuming a reorganizational energy of ∼1 eV for these through-DNA ET processes,[25] the forward CT reaction (charge injection) for both AQ and Rh will lie in the normal region, while BET will lie in the inverted region.[52] However, BET should be more inverted for AQ. Additionally, formation of a triplet ion pair with AQ will further slow BET. Thus inspection of the energetics suggests that BET should be considerably slower for AQ than for Rh.

Implications and Conclusions. These studies provide the first direct comparison of DNA CT reactions using a variety of DNA-bound photooxidants. Significant differences are apparent using the different photooxidants. These differences cannot be attributed to artifacts associated with aggregation of intercalators. Instead comparisons in assemblies using different photooxidants reveal CT characteristics of the photooxidant as well as CT characteristics of the DNA assembly. A dominating feature of the photooxidant may be its efficiency in carrying out BET. Complementary studies examining long-range CT utilizing a significantly faster trap than oxidative DNA damage highlight the importance of BET in attenuating yields of oxidative damage and relative yields at distal versus proximal sites. Results with thionine are perhaps most illustrative, where no oxidative DNA damage is observed using the slow guanine radical trap, and a complex distance dependence is observed in oxidative reactions

(48) Turro, C.; Evenzhav, A.; Bossmann, S. H.; Barton, J. K.; Turro, N. J. *Inorg. Chim. Acta* **1996**, *243*, 101−108.
(49) Armitage, B.; Yu, C.; Devadoss, C.; Schuster, G. B. *J. Am. Chem. Soc.* **1994**, *116*, 9847−9859.
(50) Steenken, S.; Jovanovic, S. V. *J. Am. Chem. Soc.* **1997**, *119*, 617−618.
(51) Driving force values for redox processes with AQ are based on calculations from ref 49 but utilize the oxidation potential of G reported[50] by Steenken and Jovanovic.
(52) Marcus, R. A.; Sutin, N. *Biochim. Biophys. Acta* **1985**, *811*, 265−322.

using a fast radical trap. The results presented here underscore that oxidative damage yields cannot be utilized alone to estimate the forward rate of DNA CT. BET should be considered as a critical parameter in characterizing long-range CT through DNA.

Supporting Information Available: HPLC profiles of dG and d^{CP}G oxidation by photoexcited thionine anaerobically. HPLC profiles of nucleoside mixtures obtained from enzymatic digestion of irradiated ^{CP}G-containing DNA assemblies functionalized with Rh, Ru, and AQ, where assemblies of Figure 1 were derivatized with ^{CP}G at the distal site. This material is available free of charge via the Internet at http://pubs.acs.org.

JA049869Y